ORIGINAL RESEARCH

Quercetin and doxorubicin co-delivery using mesoporous silica nanoparticles enhance the efficacy of gastric carcinoma chemotherapy

Jian Fang[1,*]
Shangwu Zhang[2,*]
Xiaofeng Xue[3]
Xinguo Zhu[3]
Shiduo Song[3]
Bin Wang[3]
Linhua Jiang[3]
Mingde Qin[4]
Hansi Liang[4]
Ling Gao[3]

[1]Department of General Surgery, Zhangjiagang Hospital Affiliated to Soochow University, Suzhou, Jiangsu Province, People's Republic of China; [2]Department of Emergency Surgery, The First Affiliated Hospital of Soochow University, Suzhou, Jiangsu Province, People's Republic of China; [3]Department of General Surgery, The First Affiliated Hospital of Soochow University, Suzhou, Jiangsu Province, People's Republic of China; [4]Department of General Surgery, The Stem Cell and Biomedical Material Key Laboratory of Jiangsu Province (The State Key Laboratory Incubation Base), Soochow University, Suzhou, Jiangsu Province, People's Republic of China

*These authors contributed equally to this work

Correspondence: Ling Gao
Department of General Surgery, The First Affiliated Hospital of Soochow University, 188 Shizi Street, Suzhou 215006, Jiangsu Province, People's Republic of China
Tel/fax +86 512 6778 0164
Email linggao0122@163.com

Background: Effective gastric carcinoma (GC) chemotherapy is subject to many in vitro and in vivo barriers, such as tumor microenvironment and multidrug resistance.

Materials and methods: Herein, we developed a hyaluronic acid (HA)-modified silica nanoparticle (HA-SiLN/QD) co-delivering quercetin and doxorubicin (DOX) to enhance the efficacy of GC therapy (HA-SiLN/QD). The HA modification was done to recognize overexpressed CD44 receptors on GC cells and mediate selective tumor targeting. In parallel, quercetin delivery decreased the expression of Wnt16 and P-glycoprotein, thus remodeling the tumor microenvironment and reversed multidrug resistance to facilitate DOX activity.

Results: Experimental results demonstrated that HA-SiLN/QD was nanoscaled particles with preferable stability and sustained release property. In vitro cell experiments on SGC7901/ADR cells showed selective uptake and increased DOX retention as compared to the DOX mono-delivery system (HA-SiLN/D).

Conclusion: In vivo anticancer assays on the SGC7901/ADR tumor-bearing mice model also revealed significantly enhanced efficacy of HA-SiLN/QD than mono-delivery systems (HA-SiLN/Q and HA-SiLN/D).

Keywords: gastric carcinoma, chemotherapy, quercetin, doxorubicin, co-delivery

Introduction

To date, cancer remains to be one of the most deadly diseases that lack effective treatments.[1,2] As the most widely adopted approach in cancer therapy, chemotherapy is subject to many in vitro and in vivo barriers, such as tumor microenvironment[3] and multidrug resistance (MDR).[4] Tumor microenvironment is a complicated system that comprised different types of cells, including tumor-associated fibroblasts, macrophages, and endothelial cells, which are the main components that contribute to the resistance of drug delivery approaches (DDS) and decrease the permeation, as well retention of both DDS and chemotherapeutic agents.[5] On the other hand, by continuously secreting growth-inducing cytokines and growth factors, these cells can facilitate the survival of tumor cells that further diminish the chemotherapy outcome in another way.[6,7] In particular, during the chemotherapy processes, chronic damage to stroma cells elicits the secretion of damage response program molecules to promote the survival and growth of neighboring cells, thus causing acquired MDR to the chemotherapies. Wnt16 as a member of the Wnt family has been well recognized to be one of the major mitogenic growth factors that constitute damage response program molecules.[8] It was reported that treatment-induced DNA damage in the neighboring benign stroma cells promotes chemotherapy resistance through paracrine secretion of Wnt16.[9] As a result, it was suggested

that Wnt16 might be a molecular target for remodeling the tumor microenvironment for enhanced chemotherapy.

It has been generally recognized that successful chemotherapy for cancer relies on the aid of other assistant approaches for improved bioavailability.[10–12] For the past decades, many smart DDS capable of encapsulating and targeted delivering the chemotherapeutic agents to the tumor tissue have been proposed, including organic ones such as polymeric micelles[13] and liposomes,[14] as well as inorganic candidates such as calcium carbonate,[15] gold nanoparticles,[16] and silica nanoparticles (SiLN).[17,18] Among these DDS, SiLN has been identified as a preferable carrier due to its ease of preparation, modification, as well as high drug-loading capacity and biocompatibility.[19]

Gastric carcinoma (GC) as the fourth most common cancer and the second leading cause of cancer death around the world has exerted great threat to public health.[20] Due to its recurrence and metastasis, the estimated overall 5-year survival rate of GC is merely around 15%.[21] It has been suggested in previous report that CD44 is a key molecule that participates in many cellular processes of GC cells.[22] The expression of CD44 in human GC has been identified to serve as an indispensable indicator for tumor progression, metastasis, and patient survival, and[23] it has been generally recognized that high CD44 expression was associated with poor chemotherapy outcomes.[24] As an important receptor of hyaluronic acid (HA), CD44 is overexpressed in not only human GC but also the majority of malignant cells to mediate HA-related cell adhesion and HA endocytosis.[25] Therefore, CD44 proteins have been considered as a preferable target receptor for specific drug delivery to GC.[26] In fact, HA has been widely used as a drug/gene carrier and as a surface ligand for nanoparticles to target CD44 overexpressing cells.[27–29]

Quercetin (QC) is a polyphenolic flavonoid compound, which has shown different promising biological activities, including apoptosis induction, angiogenesis inhibition, and antiproliferative action against several human carcinoma cells.[30] Besides, QC can competitively inhibit the members of MDR family, such as P-glycoprotein (P-gp), MRP1, and BCRP,[31] which are responsible for the recognition and efflux of chemical drugs. More importantly, it has also been confirmed by a previous report that QC exerts satisfactory Wnt16 knockdown efficiency in NIH3T3 murine fibroblasts.[6] Doxorubicin (DOX) is a chemotherapy medication used to treat various kinds of cancers, including breast cancer[32] and GC.[33] However, both clinical and fundamental studies have proved that the performance of DOX could be greatly impaired by MDR, especially acquired MDR, after cells have been exposed to a certain dosage of DOX.[34,35]

Combination chemotherapy for cancer therapy is considered as an important protocol to enhance therapeutic effects and reduce systemic toxicity by simultaneously modulating multiple cell-signaling pathways.[36,37] As a result, DOX is often used together with other agents to further improve its anticancer performance as well as reduce the side effects.[38,39] Co-delivering systems have been widely explored by precious works, in which polymer-based DDS, such as HA,[40] polyethylene glycol,[4] chondroitin sulfate,[36] etc have shown great promise in overcoming the abovementioned dilemma. However, compared with previous works' focus on co-delivering QC and DOX,[41,42] persistent work is still required on the fabrication of a reliable and reproducible hybrid platform with decent drug-loading capability as well as tumor targetability to enhance the co-delivering efficacy in GC chemotherapy.

In this study, HA-modified SiLN nanoparticles (HA-SiLN) were first synthesized. Then, the HA-SiLN was employed to co-load QC and DOX to finally construct QC and DOX co-delivery DDS (HA-SiLN/QD). The in vitro and in vivo performance of HA-SiLN/QD was systematically investigated on DOX-resistant human GC cell line (SGC7901/ADR) and xenograft mouse model.

Materials and methods
Materials

Triton X-100, tetraethyl orthosilicate (TEOS), N-(2-aminoethyl)-3-aminopropyltrimethoxysilane (AEAPS), dicyclohexylcarbodiimide (DCC), N-hydroxysuccinimide (NHS), QC, DOX, HA (10 kDa), MTT, and DiR were purchased from Sigma-Aldrich Co. (St Louis, MO, USA). Antibodies were purchased from Santa Cruz Biotechnology Inc (Santa Cruz, CA, USA). All other reagents were of analytical grade and used without further purification.

Cell culture

DOX-resistant human GC (SGC7901/ADR) and mouse embryonic fibroblast (NIH3T3) cells were purchased from the Cell Bank of Shanghai Institute of Biochemistry and Cell Biology (Shanghai, People's Republic of China) and cultured in Dulbecco's Modified Eagle's Medium (Sigma-Aldrich Co.) supplemented with 10% fetal bovine serum (Thermo Fisher Scientific, Waltham, MA, USA), 100 U/mL penicillin, and 100 μg/mL streptomycin (Thermo Fisher Scientific) in a cell incubator (HERAcell 150i, Thermo Fisher Scientific) with humidified atmosphere of 95% air/5% CO_2 at 37°C. All experiments were performed on cells in the logarithmic phase of growth.

Animal model

Male BALB/c nude mice (5 weeks, 20–22 g) purchased from Shanghai Laboratory Animal Center (Shanghai, People's Republic of China) were housed in the SPF α laboratory and given free access to diet and water. All procedures were conducted in compliance with NIH guidelines for care and use of research animals and approved by the ethics committee of The First Affiliated Hospital of Soochow University. The tumor-bearing mice were produced similar to the protocol in a previous report.[43] In brief, a suspension of SGC7901/ADR cells (2×10^6 cells in 0.2 mL physiological saline) was subcutaneously inoculated into the left flank and raised until the tumor reached designated volume (calculated by the formula: $W^2 \times L/2$, where W and L are the shortest and longest diameter, respectively).

Preparation and drug loading of HA-modified mesoporous SiLN (HA-SiLN)

Amine-terminated mesoporous SiLN was directly synthesized by using the synchronous hydrolysis of TEOS and AEAPS in water-in-oil microemulsion. Briefly, a water-in-oil microemulsion was prepared by mixing 1.8 mL of Triton X-100, 7.5 mL of cyclohexane, and 1.6 mL of *n*-hexanol. After stirring for 0.5 hour, 180 mL of TEOS and 60 mL of AEAPS were then added as precursors for silica matrix formation, followed by the addition of 100 μL of NH_4OH to initiate the polymerization process. The reaction was allowed to continue for 24 hours at room temperature. Afterward, additional ethanol was added with proper centrifugation (CR21G; Hitachi Ltd., Tokyo, Japan, 3,000 rpm for 10 minutes) to precipitate amine-terminated SiLN. The precipitate was washed with ethanol and water, respectively, several times to remove the surfactant and unreacted molecules.[44]

HA was chemically conjugated to amine-terminated SiLN to prepare HA-SiLN according to a previous report.[45] Briefly, 0.9 g DCC and 0.55 g NHS were dissolved in 30 mL and 5 mL of dimethyl formamide (DMF), respectively. About 0.42 g HA was dissolved in 70 mL of formamide at 50°C. In an ice bath, solutions of DCC and NHS were successively dropped into HA solution under the protection of nitrogen to activate the carboxyl group for 1 hour. In addition, 0.15 g amine-terminated SiLN was dispersed in 5 mL of DMF using probe-type sonication (Beidi-IIYJ; Nanjing Beidi Co., Ltd., Nanjing, People's Republic of China, 400 W, 30 minutes). The SiLN was added in a dropwise manner into the HA solution under the protection of nitrogen. After stirring at room temperature for 24 hours, the reaction was terminated by adding 5-fold of purified water. The mixed solution was first subjected to filtration, followed by precipitation in excess of cold acetone to obtain HA-SiLN. The product was purified by dialyzing against deionized water and collected by lyophilization.

About 0.1 g of HA-SiLN was dissolved in 3 mL of deionized water and stirred for half an hour, and QC and DOX (0.01–0.04 g) were dissolved in DMF and then added dropwise into HA-SiLN solution under probe-type sonication (100 W for 30 minutes in an ice bath). Thereafter, the solution was continually stirred for 24 hours and dual drug-loaded HA-SiLN (HA-SiLN/QD) was obtained by centrifugation (2,000 rpm for 30 minutes). The supernatant was collected to estimate QC and DOX concentration to calculate the drug-loading content using the following equation. Single drug-loaded nanoparticle (HA-SiLN/Q or HA-SiLN/D) was obtained using the same method.

$$\text{DLE (\% w/w)} = \frac{\text{Weight of loaded QC or DOX}}{\text{Weight of DDS}} \times 100\%$$

The drug content of QC was measured using a UV spectrophotometer (D800; Beckman Coulter, Inc., Brea, CA, USA) at the wavelength of 255 nm. The drug content of DOX was measured using a fluorescence spectrophotometer (RF-6000, Shimadzu, Kyoto, Japan) with excitation wavelength, emission wavelength, and slit openings set at 505, 605, and 5 nm, respectively.

Characterization of nanoparticles

The comparative Fourier-transform infrared spectroscopy (FTIR) spectrum of HA and HA-SiLN was performed on an infrared spectrometer (VERTEX 70/70V; Bruker Optik GmbH, Ettlingen, Germany). The particle size and zeta potential of nanoparticles were measured by a Dynamic Light Scattering Analyzer (Brookhaven Instruments, Holtsville, NY, USA) and a ZetaPlus Zeta Potential Analyzer (Brookhaven Instruments), respectively. The morphology of the MB-NSi nanoparticles was further visualized using transmission electron microscopy (JEM-1200; Hitachi Ltd.).

Colloidal stability and drug release assay

For colloidal stability test, the freshly prepared HA-SiLN/QD was diluted with phosphate-buffered saline (PBS, pH 7.4) or 20% serum at the volume ratio of 1:10. The change in particle size was recorded at predetermined time intervals for up to 48 hours. The release behavior of QC and DOX from HA-SiLN/QD was assessed in PBS by the dialysis

method.[15] Briefly, the HA-SiLN/QD (containing 5 mg of QC and DOX) were suspended in 3 mL of the PBS release medium and transferred into a dialysis bag (molecular weight cutoff [MWCO] 3,500 Da). The release experiments were started by placing the dialysis bag into 27 mL of PBS with 1% Tween 80 to afford the sink condition. The experiment proceeded with continuous shaking at 100 rpm at 37°C. At a predetermined time, the release medium was withdrawn for drug content analysis (as described earlier) and replaced with equal volume of fresh one.

Cytotoxicity and synergistic effects of QC and DOX

The cytotoxicity of free or drug-loaded HA/SiLN was evaluated using the standard MTT assay. SGC7901/ADR cells were seeded at 1.0×10^4 cells/well into 96-well plates and cultured until they reached 70%–80% confluence. The primary growth medium was replaced by 200 µL of fresh serum-free Dulbecco's Modified Eagle's Medium, to which free HA-SiLN or HA-SiLN/Q, HA-SiLN/D, HA-SiLN/QD was added to achieve various concentrations. The weight/weight (w/w) ratios of QC and DOX were 0.1, 0.2, 1, 5, and 10. Plates were then returned to the incubator for up to 48 hours of incubation. After this, 20 µL of 5 mg/mL MTT solution in PBS was added to each well for an additional 4 hours of incubation. Subsequently, the medium was carefully removed and replaced by 150 µL of DMSO and measured at 570 nm using a microplate reader (EL800; BioTek Instruments Inc., Winooski, VT, USA). Untreated cells were used as a control with 100% viability. The synergy effects of QC and DOX were calculated using combination index (CI).[46] In addition, apoptosis assay was performed using the Annexin V Apoptosis Detection Kit (Beyotime, Shanghai, People's Republic of China) according to the manufacturer's instructions.

In vitro intake and drug retention

For in vitro intake study, SGC7901/ADR cells were seeded in confocal dishes ($\Phi = 15$ mm; Corning Incorporated, Corning, NY, USA) at a density of 1×10^5 cells/dish and cultured overnight. To evaluate the cellular uptake and drug retention of different formulations in SGC7901/ADR cells, the dishes were then supplemented with 2 mL serum-free medium containing different concentrations of HA-SiLN/Q, HA-SiLN/D, or HA-SiLN/QD. Additionally, cells were incubated with excess of HA solution (10 mg/mL) at 37°C for 2 hours prior to nanoparticle addition. At predetermined time intervals, cells were harvested by trypsinization, resuspended in 0.5 mL of

PBS, and then subjected to quantitative analysis using flow cytometer (FCM), BD FACSCalibur™ (BD Biosciences, San Jose, CA, USA). For time-dependent DOX retention study, cells were incubated with different formulations for 8 hours. After that, the culture medium was replaced with fresh one and the cells were further incubated for additional intervals (0.5, 1, 2, 4, or 8 hours) before being subjected to FCM analysis.

Effect of QC on protein expression using Western blotting assay

The determination of the P-gp expression levels in cells was in accordance with a previous report.[47] In detail, SGC7901/ADR cells were seeded in 6-well plates at 1.5×10^5 cells/well and treated with different formulations (15 µM QC) for 48 hours. After being washed with PBS 3 times, the cells were harvested in lysis buffer (Beyotime) for 30 minutes and centrifuged at 13,000 rpm for 10 minutes, and the protein content in the supernatant was detected using a BCA protein assay (Beyotime). Equal amounts of the protein extracts (12 µg) were loaded and separated on an 8% SDS-PAGE gel and transferred onto a nitrocellulose membrane. The membrane was incubated first with 5% nonfat milk powder in TBST buffer for 1 hour to block nonspecific binding sites and then with primary antibodies for P-gp (Abcam, Cambridge, MA, USA; 1:4,000) and β-tubulin (Abcam; 1:1,000) at 4°C overnight. After being washed with TBST, the membranes were further incubated with horseradish peroxidase-labeled goat anti-rabbit or -mouse antibodies (1:1,000) at room temperature for 1 hour. Finally, the membranes were rinsed and visualized with an electrochemiluminescence detection reagent (Beyotime). Protein expression was normalized to β-tubulin.

NIH3T3 cells were treated with equal concentration of 15 µM QC. Two days later, the cells were harvested for a Western blot assay of Wnt16 expression following a similar protocol.

In vitro cytotoxicity studies on multicellular tumor spheroids (MCTS)

The establishment of SGC7901/ADR MCTS was done according to a previous report.[48] In brief, SGC7901/ADR and NIH3T3 cells were detached from monolayers, pipetted into single-cell suspensions (1.5×10^4 cells/mL), and mixed with each other (v/v, 1:1). Afterward, cells were transferred into flat-bottomed 96-well plates precoated with 2% agarose (200 µL/well). Cells were incubated for approximately 4 days, formulations were added into the spheroids by

partially (100 µL) replacing the culture medium with fresh medium-diluted formulations. The DOX concentration was fixed at 5 µg/mL. The change in spheroids was monitored using an inverted microscope every day for 4 days. The MCTS in different groups were lysed with RIPA buffer and then subjected to Western blotting assay to analyze the expression of different proteins. GAPDH was used as the internal reference. The gray scales of bands were quantitated using ImageJ software (Wayne Rasband, National Institutes of Health, Bethesda, MD, USA).

In vivo tumor targeting

To evaluate the tumor-targeting capability of HA-SiLN/QD, near-infrared probe DiR was loaded into HA-SiLN/QD during the drug-loading process to achieve DiR-labeled HA-SiLN/QD. The DiR-labeled HA-SiLN/QD was intravenously administered into the SGC7901/ADR tumor xenograft mice (tumor volume: 300 mm³, n=3) followed by investigation through a noninvasive near-infrared optical imaging system (FX PRO; Kodak, Rochester, NY, USA) for 24 hours. Mice injected with the same amount of free DiR (20 µg DiR/kg) were employed as control. Additionally, in order to further confirm the interaction between CD44 receptors and HA, mice in group 3 were intravenously injected with a high dose of free HA (1,200 mg/kg) 1 hour before being injected with DiR-labeled HA-SiLN/QD. Finally, the mice were sacrificed and the hearts, livers, spleens, lungs, kidneys, and tumors of every mouse were excised to measure their individual fluorescence intensities. Kodak Molecular Imaging Software 5.X (Kodak) was used to analyze the images.

In vivo anticancer efficiency

SGC7901/ADR tumor-bearing nude mice model was established. When the tumors reached a mean volume of approximately 100 mm³, mice were randomly assigned to 4 treatment groups (n=6): saline, HA-SiLN/QD (QC equivalent of 5 mg/kg), HA-SiLN/D (DOX equivalent of 5 mg/kg), and HA-SiLN/QD (QC and DOX were equivalent of 5 mg/kg) with reference to a previous report.[6] The treatment was implemented by intravenous injection every 2 days 7 times. Tumor volume (mm³) was calculated using the formula: tumor volume = (shortest diameter)² × (longest diameter) ×0.5. The tumor growth and body weight variation curves were plotted using the average tumor volume vs days after the first treatment. All the mice were sacrificed 14 days after the first treatment, and their tumors were resected. The excised tumors in each group were fixed using 4% paraformaldehyde buffer, embedded in paraffin, and sectioned into 5 µm thick slices. The sections were stained with hematoxylin and eosin (Beyotime) for histological examinations and imaged under an inverted microscope.

For analysis of P-gp, α-SMA, Wnt16, and Caspase 3 expression in tumor tissues, the dissected tumors were weighted and cut into pieces and lysed with RIPA buffer at 10 time volumes relative to the tumor weight, incubated on ice for 30 minutes, and sonicated for 10 minutes; they were then centrifuged at 10,000 rpm for 10 minutes. The protein content of the supernatant was quantitated using the BCA assay.

Results and discussion
Characterization of nanoparticles

FTIR analysis was performed to confirm the HA conjugation to amine-terminated SiLN (Figure S1). Afterward, the as-prepared HA-SiLN/QD (QC/DOX =1, w/w) was characterized in regard to its particles size, zeta potential, as well as morphology (Table S1). According to results obtained using a Zetasizer (Figure 1A), the size distribution of HA-SiLN/QD was located at around 100 nm with narrow distribution range, which was reflected by its relatively
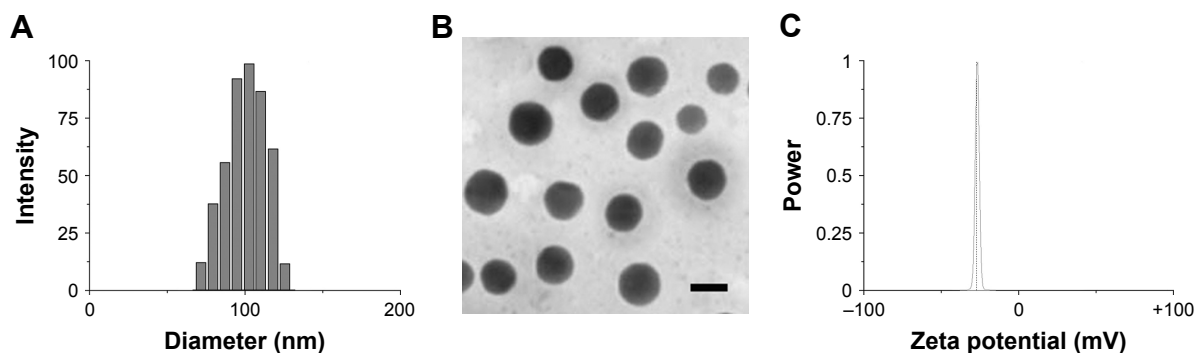

Figure 1 Particle size distribution (**A**), zeta potential (**B**) and morphology (**C**) of HA-SiLN/QD.
Note: Scale bar: 100 nm.

small polydispersion index of 0.123 (<0.3). This was also confirmed by morphology observation using transmission electron microscopy (Figure 1B). It has been reported that the high permeability of tumor tissue could facilitate the accumulation of nanoparticles, especially those with size under 200 nm, via the well-known enhanced permeability and retention effect.[3] In addition, the surface zeta potential also plays important role in dominating the in vivo fate of nanoparticles. It was well recognized that due to its hydrophilicity, HA (like PEG) can prevent opsonin adsorption by steric repulsion, leading to reduced uptake by the mononuclear phagocyte system.[25] As shown in Figure 1C, the zeta potential of HA-SiLN/QD was −28.56 mV. According to the UV and fluorescent quantitation results, the drug loading content could up to 29.7% for QC (0.297 mg QC per mg nanoparticles) and 32.6% for DOX (0.326 mg DOX per mg nanoparticles), with drug loading efficiencies of 81.6% and 85.7%, respectively. More importantly, the drug loading ratio of QC to DOX (w/w) could be well tuned by varying the charged ratios.

Colloidal stability and drug release assay

Particle size is a critical parameter to determine the in vivo fate of the DDS. As a result, stability in physiological conditions is the prerequisite requirement if a DDS is intended to safely deliver the encapsulated drug molecules to bypass

multiple extracellular barriers.[48] Herein, HA-SiLN/QD (QC/DOX =1, w/w) was studied regarding its stability as well as hemolysis as a function of time and concentration, respectively. To estimate the colloidal stability of the described DDS, the change in particle size of HA-SiLN/QD, which serves as an indicator of potential instability under physiological conditions, was monitored in PBS (pH 7.4) as well as 20% serum. As shown in Figure 2A, the size of HA-SiLN/QD remained stable with only slight fluctuation in PBS for 48 hours, which indicated that the as-prepared HA-SiLN/QD was capable of maintaining its size without being significantly affected by the environment for a relatively long time. Additional serum stability as well as long-term colloidal stability (Table S2) also confirmed the conclusion. The drug release profile of HA-SiLN/QD was investigated. As shown in Figure 2B, unlike free drugs that could be quickly diffused in a short time (50% in 4 hours and over 90% in 12 hours), both the encapsulated drugs showed a sustained release property. Different release behaviors were observed in different pH conditions. In detail, under physiological condition (pH 7.4), the HA-SiLN/QD showed relatively slow release, with approximately 30% of the encapsulated drug being released in 48 hours. However, more than 80% of the drugs in HA-SiLN/QD were being released after 48 hours of incubation in acidic environment. At the same time, the release of QC and DOX showed a similar profile with synchronized release
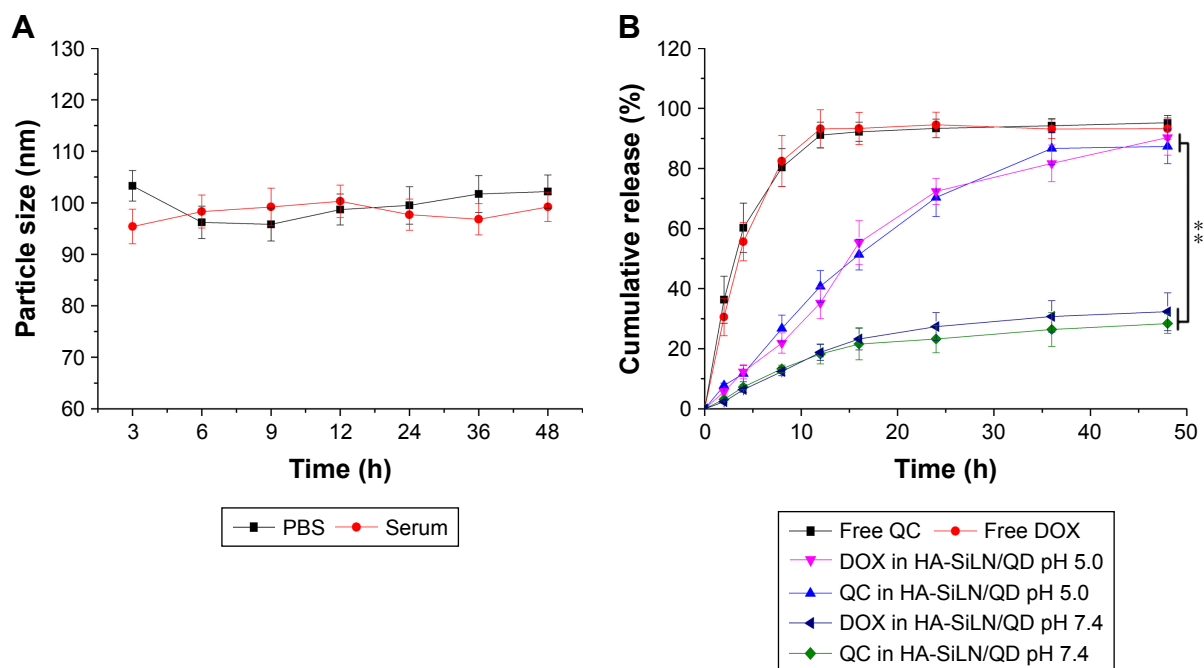

Figure 2 (**A**) Colloidal stability of HA-SiLN/QD in PBS (pH 7.4) at 37°C for up to 48 hours, (**B**) drug release profile of free QC, free DOX, and QC/DOX from HA-SiLN/QD in different pH values (7.4 and 5.5) for up to 48 hours.
Notes: Data are shown as mean ± SD (n=3). **$P<0.01$.
Abbreviations: DOX, doxorubicin; h, hours; PBS, phosphate-buffered saline; QC, quercetin.

behaviors throughout the whole experiment and was near linear before reaching a balance. The successful loading of both drugs as well as different drug release in different conditions might be able to change their in vitro and in vivo behaviors to achieve a more sustainable and targeted way which is beneficial for HA-SiLN/QD to act as a preferable DDS.

Cytotoxicity and synergistic effects of QC and DOX

The cytotoxicity effect of free HA-SiLN was first determined to verify its safety profile. As shown in Figure S2, free HA-SiLN showed negligible cytotoxicity on SGC7901/ADR cells at all tested concentrations and time intervals. Even at the highest concentration of 200 μg/mL (higher than that adopted in the following cytotoxicity assay) for 48 hours, the cell viability in HA-SiLN-treated cells still have no significant difference to that of blank ones. As a result, it was inferred that the following cytotoxicity was all attributed to the loaded drugs not the carrier.

The synergistic effects of different drug combination ratios against SGC7901/ADR cells were investigated. The optimal mass ratio of QC and DOX was evaluated using the CI. As shown in Figure 3A, the CI attained its minimum when the w/w ratio of QC and DOX reached 1, indicating

that the strongest synergistic effect was achieved. Thus, we chose the w/w ratio of 1 in the subsequent experiments. Afterward, apoptosis assay was performed to evaluate the in vitro cytotoxicity of selected HA-SiLN/QD (QC/DOX =1, w/w). As shown in Figure 3B, compared with HA-SiLN/Q and HA-SiLN/D at the same condition, HA-SiLN/QD demonstrated the highest apoptosis rate, which inferred that applying QC and DOX together might exert enhanced cytotoxicity on GC cells than administering either of them alone.

In vitro intake and drug retention

The cellular uptake profile of nanoparticles is usually characterized using fluorescence method. DOX, being a model self-illuminating fluorescent molecule, was quantitative analyzed by FCM at different time points in terms of fluorescence intensity. It has been demonstrated that the modified HA polymers exposed on the surface of the nanoparticles can target CD44, which is excessively expressed in various cancer cells.[49] In order to address the concept of HA-mediated targeting, SGC7901/ADR cells overexpressing CD44 were employed for cellular uptake evaluation.[50] As shown in Figure 4A, the fluorescence signal of HA-SiLN/QD gradually became stronger with extended incubation time, indicating that the intracellular uptake of HA-SiLN/QD happened in a time-dependent manner. As expected, after HA pretreatment, the fluorescence intensity of HA-SiLN/QD suffered a great decline. These results provided convincing evidence that HA-SiLN/QD was internalized into cells via HA-mediated endocytosis.

Furthermore, the intracellular time-dependent retention of DOX in different formulations was also determined. As depicted in Figure 4B, the intracellular DOX retention of different DOX formulations decreased with incubation time to varying degrees. Most importantly, compared with HA-SiLN/D, the HA-SiLN/QD showed the strongest retention capacity with around 50% of DOX retained inside the cells after 8 hours. It was suggested that overexpressed P-gp in MDR cells could recognize and pump the drug molecules out of the cells effectively, which results in drastically decreased intracellular drug concentrations. Our DOX retention assay suggested that HA-SiLN/QD could alleviate the efflux of DOX to reverse the MDR in SGC7901/ADR cells.
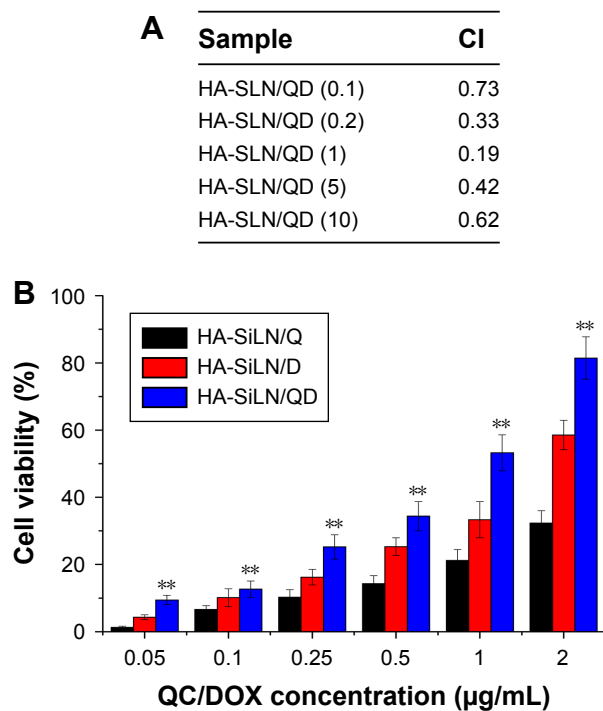
A	Sample	CI
	HA-SLN/QD (0.1)	0.73
	HA-SLN/QD (0.2)	0.33
	HA-SLN/QD (1)	0.19
	HA-SLN/QD (5)	0.42
	HA-SLN/QD (10)	0.62

Figure 3 (**A**) CI with different ratios of free QC and DOX in SGC7901/ADR cells for 48 hours, (**B**) apoptosis assay of SGC7901/ADR cells incubated with different nanoparticles at various concentrations for 48 hours.
Notes: Data are shown as mean ± SD (n=3). **$P<0.01$ vs HA-SiLN/Q and HA-SiLN/D.
Abbreviations: CI, combination index; DOX, doxorubicin; QC, quercetin.

Effect of QC on protein expression using Western blotting assay

In order to seek the potential mechanism responsible for the reverse of MDR in HA-SiLN/QD-treated SGC7901/
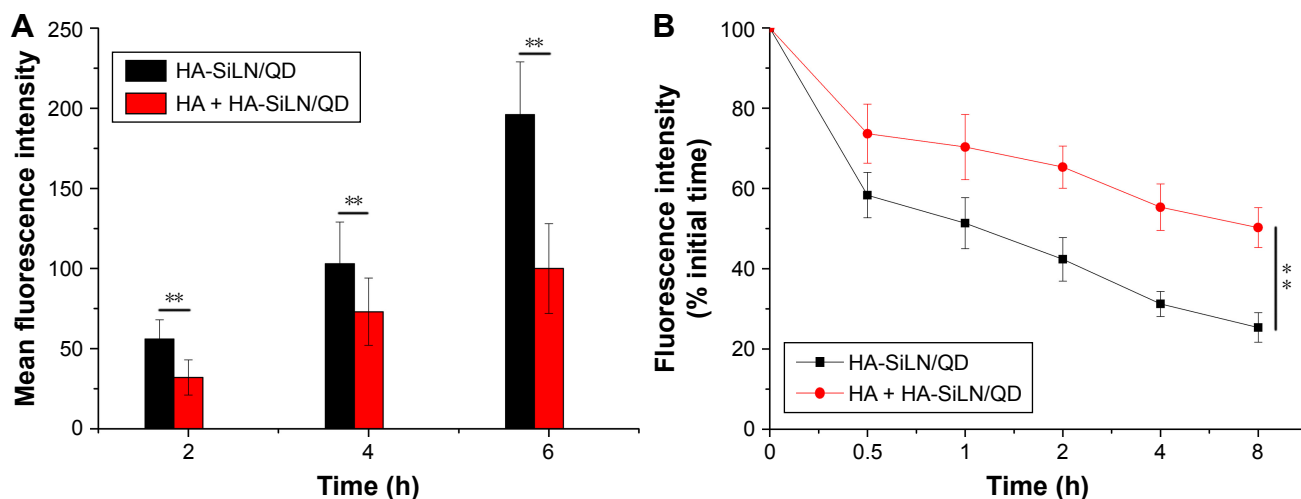
Figure 4 (**A**) Time-dependent and competitive intake of HA-SiLN/QD in SGC7901/ADR cells, (**B**) intracellular retention of DOX as a function of time.
Notes: Data are shown as mean $\pm$ SD (n=3). **$P < 0.01$.
Abbreviations: DOX, doxorubicin; HA, hyaluronic acid; h, hours.

ADR cells, the P-gp expression in different formulation-treated SGC7901/ADR cells was determined by Western blotting. The overexpression of P-gp in drug-resistant cells is one of the most significant causes of MDR, in which P-gp functions as an efflux pump transporting drugs out of cells. As shown in Figure 5A, HA-SiLN/D treatment could elevate the P-gp expression in SGC7901/ADR cells compared with the blank group, indicating that acquired MDR was involved in this process. In contrast to the HA-SiLN/D group that showed elevated P-gp level compared with the blank group, both the HA-SiLN/Q and HA-SiLN/QD groups had P-gp levels decreased by over 50%. These conclusions were also confirmed by quantitative analysis, as shown in Figure 5B. Therefore, it was believed that QC might play an important

role in the reducing the P-gp expression and increase DOX retention in SGC7901/ADR cells, which was in accordance with previous reports.[46,51]

In addition, we further explored the capability of QC in remodeling the tumor microenvironment by measuring the inhibition of Wnt16 in HA-SiLN/QD-treated NIH3T3 cells. Similar to results obtained in P-gp expression, compared with untreated cells, HA-SiLN/D could induce increased Wnt16 expression in NIH3T3 cells. As confirmed by previous report,[6] our results demonstrated that like HA-SiLN/Q, HA-SiLN/QD co-delivering QC and DOX could also significantly downregulate Wnt16 expression, indicating that QC could effectively suppress Wnt16 and remodel the tumor microenvironment to facilitate enhanced chemotherapy.
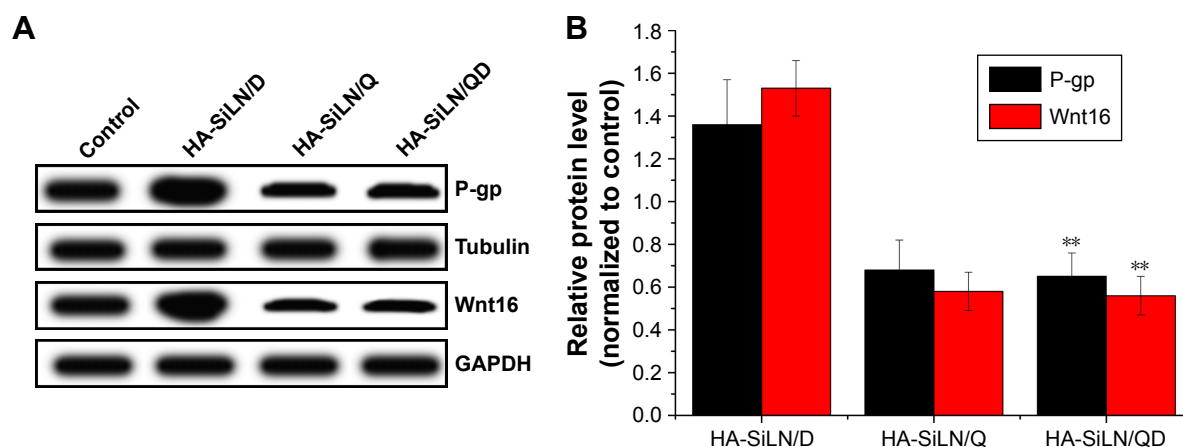

Figure 5 (**A**) Qualitative and (**B**) quantitative analyses of effects of QC on P-gp and Wnt16 expression in SGC7901/ADR cells, as determined by Western blotting analysis.
Notes: Data are shown as mean $\pm$ SD (n=3). **$P < 0.01$ vs HA-SiLN/D.
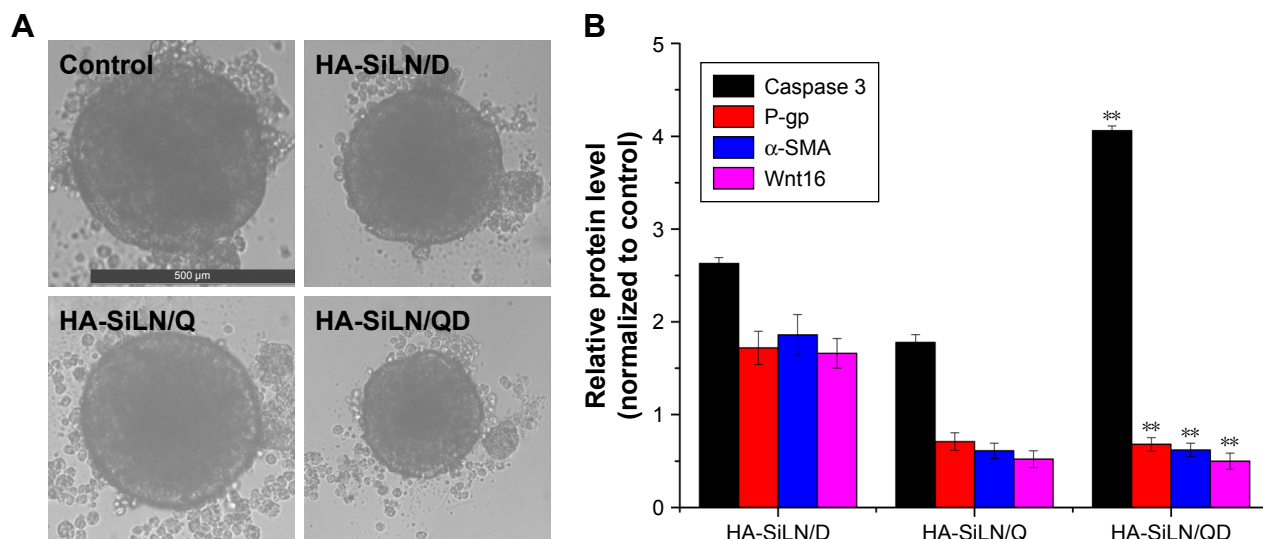**Abbreviations:** P-gp, P-glycoprotein; QC, quercetin.

Figure 6 (**A**) Representative of saline, HA-SiLN/D-, HA-SiLN/D-, and HA-SiLN/QD-treated SGC7901/ADR MCTS at 4 days postincubation, (**B**) variation of protein expression in different formulation-treated MCTS as compared to control.
Notes: Data are shown as mean ± SD (n=3). **$P<0.01$ vs HA-SiLN/D.
Abbreviations: MCTS, multicellular tumor spheroids; P-gp, P-glycoprotein.

In vitro cytotoxicity studies on MCTS

In order to further confirm the synergistic anticancer efficacy of QC and DOX, 3D SGC7901/ADR MCTS which mimicked the solid tumors was employed. As displayed in Figure 6A, after 4 days of co-incubation, the drug-containing formulations were all shown to reduce the diameter of SGC7901/ADR MCTS when compared with the control group. It is worth mentioning that HA-SiLN/QD co-delivering QC and DOX exerted the most significant reduction on diameter of SGC7901/ADR MCTS. These results suggested that the co-delivery of QC and DOX could synergistically exert their anticancer functions to achieve a better outcome.

Moreover, symbol proteins in MCTS after being treated with different formulations were quantified using Western blotting assay (Figure 6B). Caspase 3 quantification revealed that in the HA-SiLN/QD-treated MCTS, Caspase 3 level was 2.63-fold that in control groups, indicating strong cell apoptosis. In contrast, MCTS in the other 2 chemotherapy groups had much lower Caspase 3 levels. The change in the P-gp level in MCTS showed that treatment with HA-SiLN/D could trigger acquired MDR that elevate the expression of P-gp levels. However, MCTS treated with HA-SiLN/Q and HA-SiLN/QD could reverse this process with significantly decreased P-gp level. Fibroblast contents reflecting the situation of tumor microenvironment were also assessed using α-SMA and Wnt16. In line with our in vitro experiments, the number of active fibroblasts and collagen increased

significantly after HA-SiLN/D treatment, while the HA-SiLN/Q and HA-SiLN/QD treatments resulted in a drastic reduction in both fibroblasts and collagen compared to the untreated control. All these results indicated that the HA-SiLN/QD could significantly decrease the fibroblasts growth and amount of collagen in the tumors and reverse MDR, both of which contributed to enhanced chemotherapy of GC.

In vivo tumor targeting

To assess the tumor-targeting ability of HA-SiLN/QD, the biodistribution of DiR-labeled HA-SiLN/QD and free DiR in the SGC7901/ADR tumor xenograft mice was monitored using a noninvasive imaging system. As shown in Figure 7A, at 24 hours postadministration, DiR-labeled HA-SiLN/QD displayed a remarkable fluorescence signal at the tumor site. In contrast, almost no signal at the tumor site was captured at 24 hours postinjection in the free DiR group, which might be due to the rapid clearance of the low-molecular weight DiR molecule. In order to further confirm the role of HA in the active targeting of HA-SiLN to CD44 receptors of tumor, a high dose of HA polymer was intravenously injected prior to administration of DiR-labeled HA-SiLN/QD to saturate CD44 receptors on GC cells. As expected, a noticeable attenuation of fluorescence signal at the tumor site was observed, suggesting that the superior tumor targetability of HA-SiLN was significantly related to HA modification. 24 hours postinjection, all the mice were sacrificed to obtain tumors as well as major organs for ex vivo imaging.
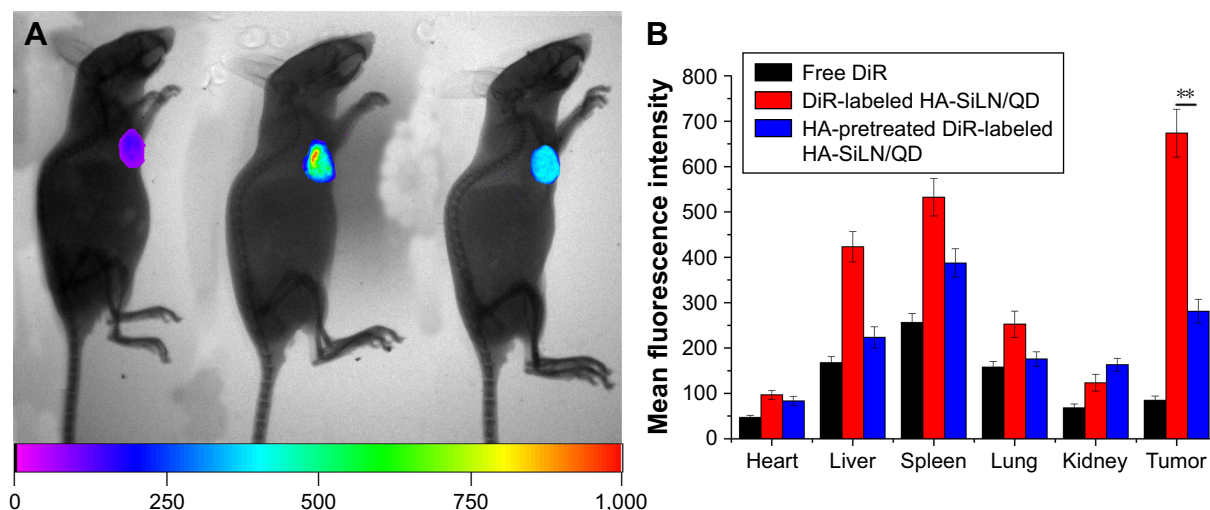
Figure 7 (**A**) In vivo distribution of free DiR, DiR-labeled HA-SiLN/QD, and HA-pretreated DiR-labeled HA-SiLN/QD at 24 hours postinjection (left: free DiR; middle: DiR-labeled HA-SiLN/QD; right: HA-pretreated DiR-labeled HA-SiLN/QD). (**B**) Region-of-interest analysis of fluorescent signals from the tumors and normal tissues. Data are shown as mean ± SD (n=3). **$P<0.01$.
Abbreviation: HA, hyaluronic acid.

As presented in Figure 7B, the strongest fluorescence signal was visualized at the tumor tissue after administration of DiR-labeled HA-SiLN/QD, compared to free DiR and HA pretreatment groups. In detail, the fluorescence intensity of DiR-labeled HA-SiLN/QD at the tumor site was 7.96-fold and 2.39-fold higher than that of free DiR and HA pretreatment groups, respectively, which further confirmed our in vivo observations.

In vivo anticancer efficiency

The in vivo therapeutic efficacy of the HA-SiLN/QD with a QC/DOX equivalent dose of 5 mg/kg was compared with that of HA-SiLN/Q, HA-SiLN/D, and saline in an SGC7901/ADR tumor xenograft model. Once the tumor volume reached 100 mm³, mice were randomly divided into 4 groups (n=6). The treatments were administered by intravenous injection every 2 days for a total of 7 treatments over a period of 14 days. As shown in Figure 8A, compared with the saline group, growth inhibition was observed in all drug-treated groups. However, due to the hostile tumor microenvironment as well as strong MDR in tumor tissues, the anticancer efficacy of the HA-SiLN/D group was very limited. Unfortunately, HA-SiLN/Q showed inferior efficacy to that of HA-SiLN/D due to the lack of an effective anticancer drug. In contrast, the HA-SiLN/QD group resulted in much better therapeutic efficacy than the other groups, which was also confirmed by hematoxylin and eosin staining, as displayed in Figure 8C. In addition, compared to the combination of free

QC and DOX, it was suggested that the superior anticancer efficacy of HA-SiLN/QD might due to CD44-based targeted delivery. Quantification of symbol proteins (Caspase 3, P-gp, α-SMA, and Wnt16) in tumor tissue (Figure 8B) also helped us reach a similar conclusion to that obtained in MCTS, which further confirmed the superiority of remodeling the TME and reversing MDR by HA-SiLN/QD.

Conclusion

We successfully developed tumor-targeted SiLN nanoparticles capable of co-delivering QC and DOX (HA-SiLN/QD) for effective GC chemotherapy. Our results demonstrated that the HA modification could recognize the overexpressed CD44 receptor on GC cells and mediate selective tumor targeting. In addition, QC could decrease the expression of Wnt16 and P-gp, thus remodeling the tumor microenvironment and reversing MDR to facilitate the functionalization of DOX. The nanoscaled HA-SiLN/QD exhibited preferable stability with sustained release property. In vitro experiments on SGC7901/ADR cells showed selective uptake via HA-mediated endocytosis. In addition, increased DOX retention as compared to the DOX mono-delivery system (HA-SiLN/D) was also observed. In vivo anticancer assays on the SGC7901/ADR tumor-bearing mice model also revealed significantly enhanced efficacy of HA-SiLN/QD than mono-delivery systems (HA-SiLN/Q and HA-SiLN/D).
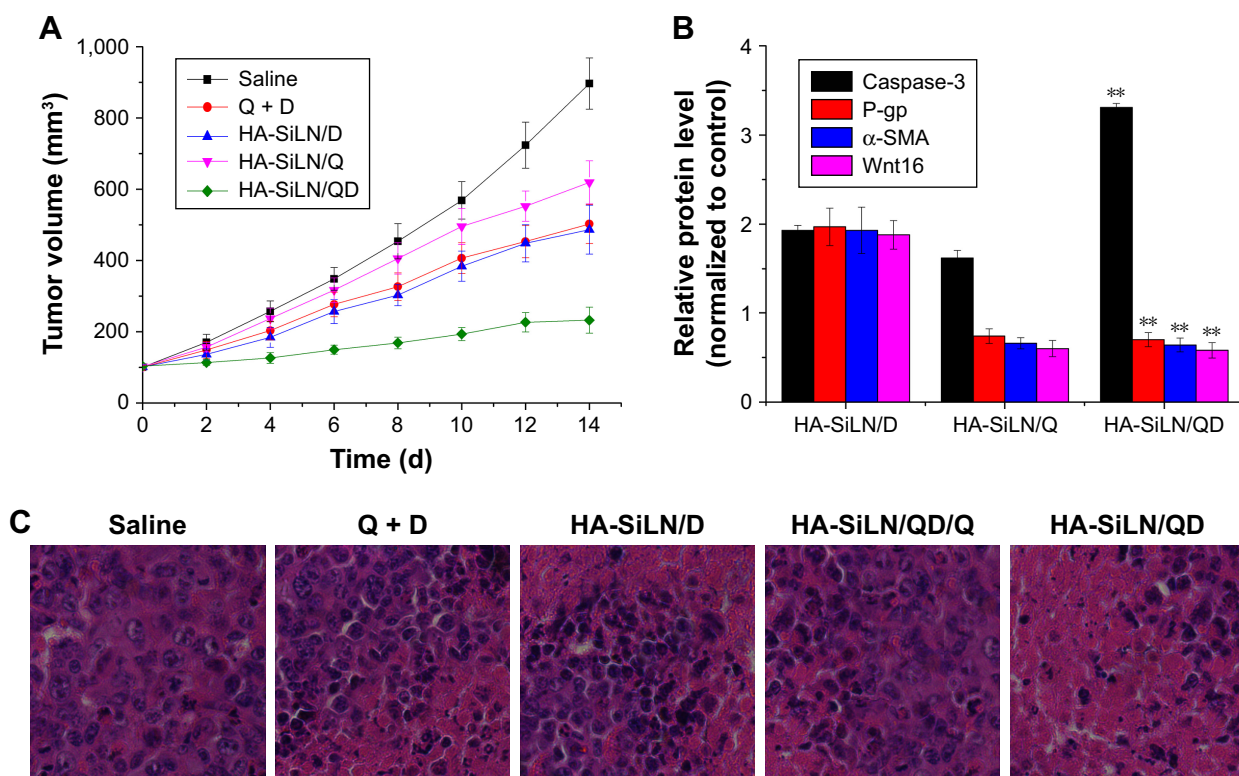
Figure 8 (**A**) The tumor volume variation of SGC7901/ADR tumor-bearing BALB/c mice after intravenous injection administration of different formulations. The treatment was implemented by intravenous injection every 2 days for 7 times at a QC/DOX dosage of 5 mg/kg. Data are expressed as mean ± SD (n=6). (**B**) Variation of protein expression in different formulation-treated tumor tissues as compared to control. Data are shown as mean ± SD (n=3). **$P<0.01$ vs HA-SiLN/D. (**C**) Hematoxylin and eosin staining images (400×) of tumor tissues from different formulation-treated groups.
Abbreviations: d, days; DOX, doxorubicin; QC, quercetin.

Disclosure

The authors report no conflicts of interest in this work.

References

1. Chen W, Zheng R, Baade PD, et al. Cancer statistics in China, 2015. *CA Cancer J Clin*. 2016;66(2):115–132.
2. Tang D, Zhao X, Yang T, Wang C. Paclitaxel prodrug based mixed micelles for tumor-targeted chemotherapy. *RSC Adv*. 2018;8(1):380–389.
3. Wang C, Chen S, Wang Y, et al. Lipase-Triggered Water-Responsive "Pandora's Box" for Cancer Therapy: Toward Induced Neighboring Effect and Enhanced Drug Penetration. *Adv Mater*. 2018;30(14):1706407.
4. Gu Y, Li J, Li Y, et al. Nanomicelles loaded with doxorubicin and curcumin for alleviating multidrug resistance in lung cancer. *Int J Nanomedicine*. 2016;11:5757–5770.
5. Ramasamy T, Haidar ZS, Tran TH, et al. Layer-by-layer assembly of liposomal nanoparticles with PEGylated polyelectrolytes enhances systemic delivery of multiple anticancer drugs. *Acta Biomater*. 2014;10(12):5116–5127.
6. Sundaramoorthy P, Ramasamy T, Mishra SK, et al. Engineering of caveolae-specific self-micellizing anticancer lipid nanoparticles to enhance the chemotherapeutic efficacy of oxaliplatin in colorectal cancer cells. *Acta Biomater*. 2016;42:220–231.
7. Ramasamy T, Ruttala HB, Sundaramoorthy P, et al. Multimodal selenium nanoshell-capped Au@mSiO2 nanoplatform for NIR-responsive chemo-photothermal therapy against metastatic breast cancer. *NPG Asia Mater*. 2018;10(4):197–216.
8. Abbad S, Wang C, Waddad AY, Lv H, Zhou J, Preparation ZJ. Preparation, in vitro and in vivo evaluation of polymeric nanoparticles based on hyaluronic acid-poly(butyl cyanoacrylate) and D-alpha-tocopheryl polyethylene glycol 1000 succinate for tumor-targeted delivery of morin hydrate. *Int J Nanomedicine*. 2015;10:305–320.
9. Zununi Vahed S, Salehi R, Davaran S, Sharifi S. Liposome-based drug co-delivery systems in cancer cells. *Mater Sci Eng C Mater Biol Appl*. 2017;71:1327–1341.
10. Wang C, Chen S, Yu Q, Hu F, Yuan H. Taking advantage of the disadvantage: employing the high aqueous instability of amorphous calcium carbonate to realize burst drug release within cancer cells. *J Mater Chem B*. 2017;5(11):2068–2073.
11. Li M, Li Y, Huang X, Lu X. Captopril-polyethyleneimine conjugate modified gold nanoparticles for co-delivery of drug and gene in anti-angiogenesis breast cancer therapy. *J Biomater Sci Polym Ed*. 2015;26(13):813–827.
12. Wan J, Wu W, Zhang R, Liu S, Huang Y. Anti-EGFR antibody conjugated silica nanoparticles as probes for lung cancer detection. *Exp Ther Med*. 2017;14(4):3407–3412.

13. Zheng T, Wang A, Hu D, Wang Y. Tumor-targeting templated silica nanoparticles as a dual-drug delivery system for anti-angiogenic ovarian cancer therapy. *Exp Ther Med*. 2017;14(3):2162–2170.

14. Wu H, Zhao Y, Mu X, et al. A silica-polymer composite nano system for tumor-targeted imaging and p53 gene therapy of lung cancer. *J Biomater Sci Polym Ed*. 2015;26(6):384–400.

15. Jemal A, Bray F, Center MM, Ferlay J, Ward E, Forman D. Global cancer statistics. *CA Cancer J Clin*. 2011;61(2):69–90.

16. Chen Y, Fu Z, Xu S, et al. The prognostic value of CD44 expression in gastric cancer: a meta-analysis. *Biomed Pharmacother*. 2014;68(6):693–697.

17. Bao W, Fu H–J, Xie Q–S, et al. HER2 Interacts With CD44 to Up-regulate CXCR4 via Epigenetic Silencing of microRNA-139 in Gastric Cancer Cells. *Gastroenterology*. 2011;1416(6):2076–2087.

18. Pályi-Krekk Z, Barok M, Isola J, Tammi M, Szöllosi J, Nagy P. Hyaluronan-induced masking of ErbB2 and CD44-enhanced trastuzumab internalisation in trastuzumab resistant breast cancer. *Eur J Cancer*. 2007;43(16):2423–2433.

19. Yoon C, Park DJ, Schmidt B, et al. CD44 expression denotes a subpopulation of gastric cancer cells in which Hedgehog signaling promotes chemotherapy resistance. *Clin Cancer Res*. 2014;20(15):3974–3988.

20. Yang Z, Luo H, Cao Z, et al. Dual-targeting hybrid nanoparticles for the delivery of SN38 to Her2 and CD44 overexpressed human gastric cancer. *Nanoscale*. 2016;8(22):11543–11558.

21. Ponta H, Sherman L, Herrlich PA. CD44: from adhesion molecules to signalling regulators. *Nat Rev Mol Cell Biol*. 2003;4(1):33–45.

22. Li R, Liu T, Wang K. Hyaluronic modified and amine-functionalized silica nanoparticles as intracellular siRNA delivery carriers in lung. *Cancer Gene Therapy*. 2016;9(6):10191–10200.

23. Li R, Liu T, Wang K. Hyaluronic acid-modified zirconium phosphate nanoparticles for potential lung cancer therapy. *Biomedizinische Technik Biomedical Engineering*. 2016;62(1):67–73.

24. Wang Z, Tian Y, Zhang H, et al. Using hyaluronic acid-functionalized pH stimuli-responsive mesoporous silica nanoparticles for targeted delivery to CD44-overexpressing cancer cells. *Int J Nanomedicine*. 2016;11:6485–6497.

25. Correia AL, Bissell MJ. The tumor microenvironment is a dominant force in multidrug resistance. *Drug Resist Updat*. 2012;15(1–2):39–49.

26. Hu K, Miao L, Goodwin TJ, Li J, Liu Q, Huang L. Quercetin Remodels the Tumor Microenvironment To Improve the Permeation, Retention, and Antitumor Effects of Nanoparticles. *ACS Nano*. 2017;11(5):4916–4925.

27. Trédan O, Galmarini CM, Patel K, Tannock IF. Drug resistance and the solid tumor microenvironment. *J Natl Cancer Inst*. 2007;99(19):1441–1454.

28. Niehrs C, Acebron SP. Mitotic and mitogenic Wnt signalling. *Embo J*. 2012;31(12):2705–2713.

29. Sun Y, Campisi J, Higano C, et al. Treatment-induced damage to the tumor microenvironment promotes prostate cancer therapy resistance through WNT16B. *Nat Med*. 2012;18(9):1359–1368.

30. Minaei A, Sabzichi M, Ramezani F, Hamishehkar H, Samadi N. Co-delivery with nano-quercetin enhances doxorubicin-mediated cytotoxicity against MCF-7 cells. *Mol Biol Rep*. 2016;43(2):99–105.

31. Ravishankar D, Rajora AK, Greco F, Osborn HM. Flavonoids as prospective compounds for anti-cancer therapy. *Int J Biochem Cell Biol*. 2013;45(12):2821–2831.

32. Chakravarty G, Mathur A, Mallade P, et al. Nelfinavir targets multiple drug resistance mechanisms to increase the efficacy of doxorubicin in MCF-7/Dox breast cancer cells. *Biochimie*. 2016;124:53–64.

33. Wu H, Liu S, Gong J, et al. VCPA, a novel synthetic derivative of α-tocopheryl succinate, sensitizes human gastric cancer to doxorubicin-induced apoptosis via ROS-dependent mitochondrial dysfunction. *Cancer Lett*. 2017;393:22–32.

34. Shi J, Su Y, Liu W, Chang J, Zhang Z. A nanoliposome-based photoactivable drug delivery system for enhanced cancer therapy and overcoming treatment resistance. *Int J Nanomedicine*. 2017;12:8257–8275.

35. Zhou Y, Wang S, Ying X, et al. Doxorubicin-loaded redox-responsive micelles based on dextran and indomethacin for resistant breast cancer. *Int J Nanomedicine*. 2017;12:6153–6168.

36. Wang C, Li M, Yang T, et al. A self-assembled system for tumor-targeted co-delivery of drug and gene. *Mater Sci Eng C Mater Biol Appl*. 2015;56:280–285.

37. Conde J, Oliva N, Zhang Y, Artzi N. Local triple-combination therapy results in tumour regression and prevents recurrence in a colon cancer model. *Nat Mater*. 2016;15(10):1128–1138.

38. Jiang D, Wang M, Wang T, Zhang B, Liu C, Zhang N. Multifunctionalized polyethyleneimine-based nanocarriers for gene and chemotherapeutic drug combination therapy through one-step assembly strategy. *Int J Nanomedicine*. 2017;12:8681–8698.

39. Wu C, Xu J, Hao Y, et al. Application of a lipid-coated hollow calcium phosphate nanoparticle in synergistic co-delivery of doxorubicin and paclitaxel for the treatment of human lung cancer A549 cells. *Int J Nanomedicine*. 2017;12:7979–7992.

40. Wang T, Yu X, Han L, Liu T, Liu Y, Zhang N. Tumor microenvironment dual-responsive core-shell nanoparticles with hyaluronic acid-shield for efficient co-delivery of doxorubicin and plasmid DNA. *Int J Nanomedicine*. 2017;12:4773–4788.

41. Ramasamy T, Ruttala HB, Gupta B, et al. Smart chemistry-based nano-sized drug delivery systems for systemic applications: A comprehensive review. *J Control Release*. 2017;258:226–253.

42. Ramasamy T, Ruttala HB, Chitrapriya N, et al. Engineering of cell microenvironment-responsive polypeptide nanovehicle co-encapsulating a synergistic combination of small molecules for effective chemotherapy in solid tumors. *Acta Biomater*. 2017;48:131–143.

43. Wang C, Bao X, Ding X, et al. A multifunctional self-dissociative polyethyleneimine derivative coating polymer for enhancing the gene transfection efficiency of DNA/polyethyleneimine polyplexes in vitro and in vivo. *Polym Chem*. 2015;6(5):780–796.

44. He X, Wu X, Wang K, Shi B, Hai L. Methylene blue-encapsulated phosphonate-terminated silica nanoparticles for simultaneous in vivo imaging and photodynamic therapy. *Biomaterials*. 2009;30(29):5601–5609.

45. Xiong H, du S, Ni J, Zhou J, Yao J. Mitochondria and nuclei dual-targeted heterogeneous hydroxyapatite nanoparticles for enhancing therapeutic efficacy of doxorubicin. *Biomaterials*. 2016;94:70–83.

46. Zhang Z, Xu S, Wang Y, et al. Near-infrared triggered co-delivery of doxorubicin and quercetin by using gold nanocages with tetradecanol to maximize anti-tumor effects on MCF-7/ADR cells. *J Colloid Interface Sci*. 2018;509:47–57.

47. Ye M, Han Y, Tang J, et al. A Tumor-Specific Cascade Amplification Drug Release Nanoparticle for Overcoming Multidrug Resistance in Cancers. *Adv Mater*. 2017;29(38):1702342.

48. Ding X, Xu X, Zhao Y, et al. Tumor targeted nanostructured lipid carrier co-delivering paclitaxel and indocyanine green for laser triggered synergetic therapy of cancer. *RSC Adv*. 2017;7(56):35086–35095.

49. Yang RM, Fu CP, Fang JZ, et al. Hyaluronan-modified superparamagnetic iron oxide nanoparticles for bimodal breast cancer imaging and photothermal therapy. *Int J Nanomedicine*. 2017;12:197–206.

50. Zhou L, Shang Y, Liu C, et al. Overexpression of PrPc, combined with MGr1-Ag/37LRP, is predictive of poor prognosis in gastric cancer. *Int J Cancer*. 2014;135(10):2329–2337.

51. Wang X, Chen Y, Dahmani FZ, Yin L, Zhou J, Yao J. Amphiphilic carboxymethyl chitosan-quercetin conjugate with P-gp inhibitory properties for oral delivery of paclitaxel. *Biomaterials*. 2014;35(26):7654–7665.
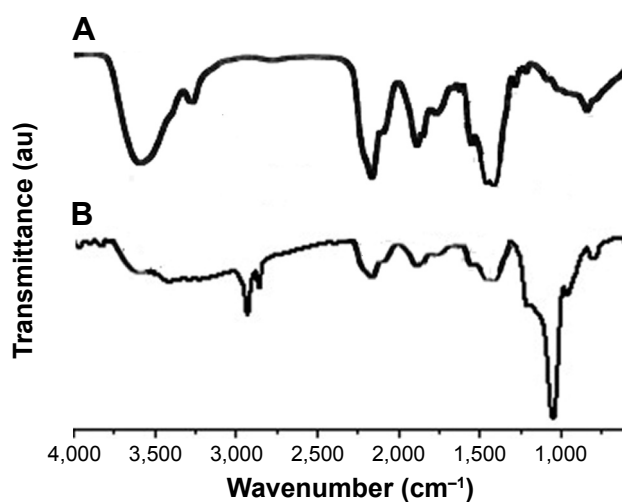
Supplementary materials

Figure S1 Comparative FTIR spectrum of HA (**A**) and HA-SiLN (**B**).
Abbreviations: FTIR, Fourier-transform infrared spectroscopy; HA, hyaluronic acid.

Table S1 Particle size, zeta potential, and polydispersity index of different nanoparticles

Formulation	Size (nm)	Zeta potential (mV)	Polydispersity index
SLN	92.61±4.12	30.6±2.83	0.216±0.08
HA-SLN	102.3±2.62	−29.9±3.12	0.116±0.05
HA-SLN/QD	101.6±3.21	−28.56±2.31	0.123±0.06
HA-SLN/DiR	102.8±2.85	−29.3±2.25	0.112±0.03

Table S2 Long-term colloidal stability (2 weeks) of HA-SiLN/QD stored at 4°C and room temperature

Condition	Size (nm) (before/after)	Zeta potential (mV) (before/after)	Polydispersity index (before/after)
4°C	101.6/102.1	−28.56/−27.43	0.123/0.126
Room temperature	101.6/103.4	−28.56/−27.17	0.123/0.145
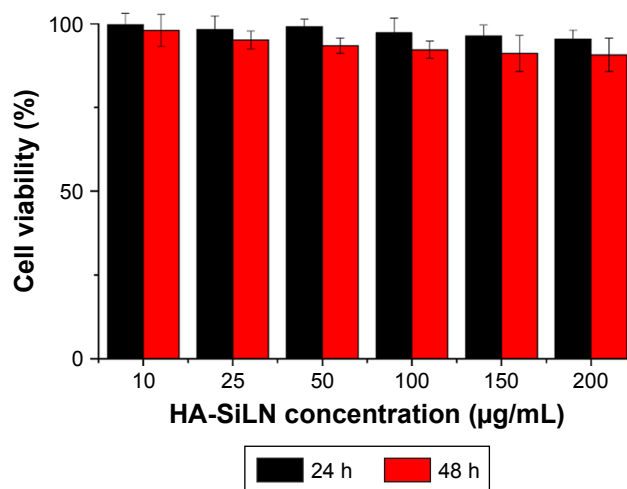
Figure S2 Cell viabilities of SGC7901/ADR cells incubated with free HA-SiLN at various concentrations for 24 and 48 hours.
Note: Data are shown as mean ± SD (n=3).